Sustainable Food Technology

ROYAL SOCIETY OF CHEMISTRY

PAPER

View Article Online
View Journal | View Issue

Cite this: *Sustainable Food Technol.*, 2024, **2**, 1506

Explicating the effect of extraction methods on the techno-functional, structural, and *in vitro* prebiotic potential of soluble dietary fibers from mango and pomegranate peel

Shriya Bhatt[ab] and Mahesh Gupta *[ab]

Peel is a major bio-waste and a potential source of numerous bioactive molecules, creating immense environmental issues but no commercial significance. Thus, different extraction conditions, including chemical, enzymatic, ultrasonication, microwave, and homogenization, with varied sample concentrations at 2%, 5%, and 10% (w/v) were employed for maximum soluble dietary fiber (SDF) extraction from both mango (Totapuri and Safeda) and pomegranate (Bhagwa and Daru) peel. The maximum SDF yield of 29.26 ± 0.25% was observed at 5% w/v for homogenization-assisted enzymatic extraction (HEE) from mango peel (Safeda). The proximate and techno-functional properties of SDF exhibited efficient activity with enhanced thermal stability and structural characteristics. Scanning electron microscopy revealed a loosened and porous structure. In addition, the samples demonstrated significant prebiotic activity with the synthesis of three major short-chain fatty acids (SCFAs) in the order of propionic (3.60 ± 0.08 mg mL^{-1}) > acetic (2.64 ± 0.01 mg mL^{-1}) > butyric acid (1.27 ± 0.01 mg mL^{-1}), as quantified *via* ultra-performance liquid chromatography (UPLC). Thereby, this study highlights the role of waste fruit peel as a potent source of SDF, exhibiting profound prebiotic activity with imminent industrial application.

Received 30th November 2023
Accepted 5th July 2024

DOI: 10.1039/d3fb00227f

rsc.li/susfoodtech

Sustainability spotlight

The present study provides substantial evidence to highlight the role of waste fruit peel as a potential source of SDF, exhibiting prebiotic activity with imminent industrial application. The study intended to decipher the knowledge for viable and reproducible methods having maximum soluble dietary fiber extraction yield with enhanced chemical and structural characteristics. The results highlight the potential role of extraction methods (homogenization and ultrasonication) as an effectual technique in augmenting the overall structural, thermal, and prebiotic properties of SDF with possible application in food product development. Consequently, the current research provides substantial evidence to highlight the role of waste fruit peel as a potential source of SDF, exhibiting prebiotic activity with imminent industrial application.

Introduction

Fruits play a crucial role in sustaining a balanced lifestyle by delivering diverse essential nutrients to the body. In this case, the demand and production of fruits have increased considerably in the recent years.[1] However, the production and processing of fruits generate waste, creating serious environmental concerns. Mango and pomegranate are two major fruits, generating about 15–20% and 40–50% of their waste in the form of a peel with no commercial significance.[2,3] This waste is a potential source of numerous bioactive molecules, importantly dietary fiber (DF).[3]

DF, a 7th fundamental nutrient, is generally classified as soluble dietary fiber (SDF) and insoluble dietary fiber (IDF) based on its solubility in water.[4] The former has been earlier reported for its ability to bind toxic molecules, reduce blood glucose levels, and proliferate intestinal microbes with the prevention of diabetes and cardiovascular diseases.[5–7] However, for a high-quality DF, the SDF content should not be less than 10%, providing effective processing characteristics along with positive health benefit.[8] Consequently, there has been a continuous effort toward identifying optimum extraction techniques with a higher SDF yield.

The extraction of SDF is generally carried out using various conventional and non-conventional techniques,[9] including thermal, enzymatic, chemical, chemo-enzymatic, ultrasonication, homogenization, and microwave-assisted extractions. According to literature reports, the dietary fiber from mango peel ranges from 28% to 78% with 13–28% of SDF and

[a]*CSIR-Institute of Himalayan Bioresource Technology, Palampur-176061, Himachal Pradesh, India. E-mail: mgupta@ihbt.res.in*

[b]*Academy of Scientific and Innovative Research (AcSIR), Ghaziabad-201002, India*

14–50% of IDF. Similarly, the dietary fiber content in pomegranate peel ranges from 33% to 62% with an SDF content of 24.78%.[10,11] However, DF from varied sources exhibits diverse yields, physicochemical, and functional properties, which entirely depend on the chemical composition and extraction method. Nowadays, the research focus mainly relies on the utilization of newer technologies, namely ultrasonication, homogenization, and microwave-assisted extraction. To the best of our knowledge, there have been no reports on comparing the effect of different extraction techniques on the yield, techno-functional, nutritional, structural, and prebiotic potential of soluble dietary fiber (SDF) extracted from mango and pomegranate fruit peels with molecular weight determination using MALDI-TOF/TOF-MS/MS.

Therefore, the aim of this study was to estimate the effect of chemical (acid, alkali), enzymatic (cellulase, α-amylase, protease, and amyloglucosidase), chemo-enzymatic, along with ultrasonication, homogenization, and microwave-assisted extractions on the structural and techno-functional properties of SDF. In addition, the *in vitro* proliferation of various probiotics was evaluated, along with the determination of major SCFAs. Overall, the study intended to interpret the knowledge for viable and reproducible methods having maximum extraction yield, along with effective prebiotic potential, generating the idea for the valorisation of waste to a potential bioactive ingredient.

Materials and methods

Material

Two mango varieties, *i.e.*, Totapuri (A), Safeda (B), and two pomegranate varieties, *i.e.*, Bhagwa (C), and Daru (D), were purchased from Himachal Pradesh Palampur (1472 meters), India (32.1109° N, 76.5363° E). The total dietary fiber kit (K-TDFR, 200A) was obtained from Megazyme (Wicklow, Ireland). The standards were from Sigma-Aldrich, India. The other chemicals and reagents were of analytic grade.

The four bacterial strains, namely *Wisella ciberia*, *Lactobacillus plantarum*, *Lactobacillus brevis*, and *Lactobacillus fermentum*, were isolated previously in the laboratory, and WOW probiotic (a mixed consortium of 19 different *Lactobacilli* and *Bifidobacteria*) was procured from Palampur market, Himachal Pradesh, India.

Soluble dietary fiber extraction from peel

Pretreatment of samples. The pretreatment of peel powder was done, as reported earlier by Bhatt *et al.*, 2022.[12]

Extraction of soluble dietary fiber. The SDF extraction was done using pre-treated peel powder (PW) with nine different methods and varied concentrations at 2%, 5%, and 10% sample-to-solvent ratios (Fig. 1A). The acid and microwave-assisted extraction (AE & MWE) of all samples was done using the method described by Li *et al.*, 2014.[13] In brief, for AE, PW was treated with sulphuric acid solution 1 N (pH 2.0), stirred at 80 °C (4 h), filtered and precipitated with 95% ethanol (three volumes). The precipitates were further centrifuged and lyophilized to get the SDF. In MWE, PW was extracted using AE, followed by MWE at 550 W for 2 min and then filtered, precipitated and lyophilized. Hot water extraction (HWE) was done, as explained by Bello *et al.*, 2018.[14] Briefly, PW was boiled at 100 °C (1 h) with stirring (150 rpm), then filtered, precipitated and lyophilized to get SDF. Similarly, alkali and ultrasound-assisted alkali extractions (ALE & UAE) were followed by the method reported by Zhang *et al.*, 2017.[15] For ALE, PW was dispersed in 1% NaOH solution (pH 9.0), incubated at 50 °C (30 min), filtered, precipitated and lyophilized to get SDF. In UAE, a similar methodology of ALE before filtration was followed, and then ultrasonication was carried out at 37 kHz at 55 °C for 15 min. After that, the sample was filtered, precipitated and lyophilized to get SDF. Ultrasonic extraction (UE) was performed, as described by Kurek *et al.*, 2018,[16] where PW was initially dispersed in phosphate buffer, pH 6.8 (20 mM), further sonicated at 37 kHz at 55 °C for 15 min, filtered, precipitated and lyophilized. Enzymatic extraction (EE) was achieved using the method reported by Cheng *et al.*, 2017,[17] following extraction *via* cellulase treatment. Briefly, PW was dispersed in water (pH 4.5), and adjusted using 1 N HCl. Thereafter, the addition of cellulase was followed by incubation with stirring at 50 °C for 4 h. Then, α-amylase (pH 5.5) was sequentially added, following incubation at 95 °C for 30 min, followed by the addition of

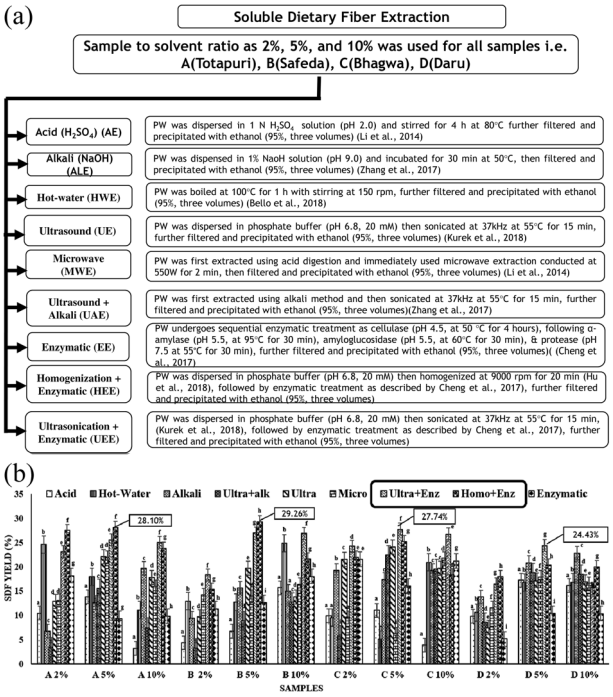

Fig. 1 (A) Extraction of soluble dietary fiber using varied sample concentration and extraction conditions. PW: pre-treated peel powder. (B) Extraction yield of soluble dietary fiber. (A) Totapuri, (B) Safeda, (C) Bhagwa, and (D) Daru, 2%, 5%, and 10% indicate the sample concentration, acid: sulphuric acid (AE), alkali: sodium hydroxide (ALE), Ultra+Alk: ultrasound-assisted alkali extraction (UAE), ultra: ultrasound (UE), micro: microwave (MWE), Ult+Enz: ultrasound-assisted enzymatic extraction (UEE), Homo+Enz: homogenization-assisted enzymatic extraction (HEE). Values are the average of three replicates ± SD with significant difference ($p < 0.05$) indicated with different letters.

amyloglucosidase (pH 5.5) at 60 °C for 30 min. Finally, protease (pH 7.5) was added at 55 °C for 30 min. The sample was then filtered, precipitated and lyophilized to get SDF. Ultrasound-assisted enzymatic extraction (UEE) was carried out with some minor modifications. In brief, UE was carried out using a method described by Kurek *et al.*, 2018,[16] as explained above, followed by EE reported by Cheng *et al.*, 2017.[17] Homogenization-assisted enzymatic extraction (HEE) was performed, following the method elucidated by Hu *et al.*, 2018,[5] with some minor modifications. In brief, PW was mixed with phosphate buffer (pH 6.8, 20 mM) and homogenized at 9000 rpm for 20 min, with EE carried out using the protocol explained by Cheng *et al.*, 2017,[17] as described above.

The yield was calculated as described in the equation below:

$$\text{SDF yield (\%)} = (X - Z - T)/Y \times 100$$

here, X signifies the weight of the extracted samples (g), Z represents the amount of ash (g), T indicates the amount of protein, and Y represents the initial sample weight (g). Finally, the sample with the maximum extraction yield was further analysed for various physicochemical and structural characteristics.

Proximate composition

The method described by Bhatt *et al.*, 2021,[18] was performed to estimate the moisture, fat, ash, and protein content. SDF was estimated using K-TDFR, 200A (Megazyme kit), following 991.43 AOAC methodology.

Techno-functional and other characteristic properties

The methodology described by Dong *et al.*, 2020,[8] was followed for the oil absorption index (OAI), water solubility index (WSI), water absorption index (WAI), emulsion stability (ES), and emulsifying capacity (EC). The previously reported method by Kumari *et al.*, 2021,[20] was followed for water activity.

The other characteristic properties, including the cholesterol-binding capacity (CBC), glucose adsorption capacity (GAC), sodium cholate binding capacity (SCBC), and cation exchange capacity (CEC), were determined as performed by Bhatt *et al.*, 2022.[12]

Sugar profile

The monosaccharide composition of samples was quantified using high-performance anion-exchange chromatography-pulsed amperometric detection (HPAEC-PAD). Initially, the hydrolysis of samples was done following the method explained by Dong *et al.*, 2020.[8] The samples were further extracted using solid–liquid extraction without derivatization. Briefly, 10 mg sample was mixed with 1.5 mL distilled water (dH_2O) and vortexed. Upon the addition of Carrez II (0.2 mL), the sample was mixed and vortexed (5 min), and then centrifuged for 20 min at 12 000 rpm. The supernatant was transferred promptly to another tube. Afterwards, the second extraction was carried out using similar steps. The supernatant of both extractions was mixed to get the final aliquot. The HPAEC coupled to 945 Professional Detector Vario, an amperometric detector (Metrohm AG, Herisau, Suiza) in pulsed amperometric mode was used to analyse the monosaccharide composition of each sample. The separation of the standards, namely inositol, glucose, fructose, xylose, sucrose, and raffinose, and the samples was carried out using a Metrosep Carb 2 – 250/4.0 column programmed at 30 ± 0.1 °C. The mobile phase (isocratic) of 10 mM L^{-1} NaAc and 100 mM L^{-1} NaOH was followed at a flow rate of 0.5 mL min^{-1}, with an injection volume of 20 μL and pressure of 15 MPa. The software A. MagIC Net (version 3.2) was used to analyse the samples.

Determination of the molecular weight using MALDI-TOF/TOF-MS/MS

The determination of the molecular weight was carried out using MALDI-TOF/TOF-MS/MS (Bruker, Ultraflextrame, USA). The sample preparation was done as defined by Lopez Garcia *et al.*, 2016,[19] with minor amendments. In brief, the 10 mg sample was dispersed in 1 mL dH_2O and sonicated for 30 min, followed by centrifugation for 20 min at 8000 rpm. The supernatant was withdrawn and stored at 4 °C in glass vials until further analysis.

Two matrixes, namely 2,5-dihydroxybenzoic acid (DHB) and 2′,4′,6′-trihydroxyacetophenone monohydrate (THAP), were used for analysis of samples. Each matrix of 10 mg mL^{-1} was dissolved in acetonitrile : water (80 : 20) prepared in 0.1% trifluoroacetic acid. 0.1 μL of sample and matrix (1 : 1) solution was loaded on the ATP Anchor Chip plate. Thereafter, the plate was allowed to dry at 37 °C for 10 min. Polytool software (Bruker Daltonics Inc., Germany) was used for the determination of the repeat unit, residue, the number of the average molecular weight (M_n), weight average molecular weight (M_w), and polydispersity index (PI). The TOF/TOF spectra were obtained at 2500 shots per spot with reflector positive ion mode within the mass range from 700 to 2000 Da.

Scanning electron microscopy (SEM) analysis

The sample mounting was carried out on the stub (aluminium stub) covered with carbon tape to carry out SEM analysis. The stubs thereafter were placed in the ion sputter (E1010 Hitachi, Japan). For conductivity, the samples were coated for 20 s with gold at a 10 Pa vacuum level. Finally, images were then analysed on SEM (S3400N; Hitachi) at 15 kV.

Fourier transformation infrared spectroscopy (FT-IR) analysis

The structural characterization of the SDF samples was carried out *via* FT-IR spectroscopy (Shimadzu). The powdered sample (10 mg) was assessed in the 400–4000 cm^{-1} spectral range, and analysed with a maximum of 16 individual scans for each sample.

Thermogravimetric (TGA) analysis

The thermal stability of all SDF samples was carried out using a TGA analyzer (NETZSCH Geratebau GmbH STA 449 F1 Jupiter) machine. In brief, 20 mg of sample was investigated in the

nitrogen atmosphere *via* TGA with temperature ranging from 20 to 400 °C at 10 °C min^{-1} heating rate.

Determination of flavonoid, phenolic content and antioxidant assays

The quantification of the total flavonoid and phenolic contents, along with antioxidant assays including 2,2-diphenyl-1-picrylhydrazyl (DPPH), 2,2′-azino-bis (3-ethylbenzothiazoline-6-sulphonic acid) (ABTS), were carried out as explained by Bhatt *et al.*, 2021.[21]

Colour assessment

A Hunter colorimeter (Chroma-Meter CR-400, KONICA MINOLTA) was used for the colorimetric assessment of samples. All of the experiments were performed in triplicate.

Prebiotic potential

α-Amylase and gastric juice hydrolysis activity. The α-amylase and gastric juice hydrolysis activity was performed, as defined earlier by Bhatt *et al.*, 2020.[22]

In vitro prebiotic activity

Probiotic strains, namely *Wisella ciberia*, *Lactobacillus plantarum*, *Lactobacillus brevis*, and *Lactobacillus fermentum*, along with WOW probiotic, were used to assess the prebiotic potential of various SDF samples at different time intervals (24 h and 48 h). The method described by Chen *et al.*, 2020,[23] was followed to evaluate the prebiotic potential of SDF samples on the proliferation of various probiotics. The bacterial growth calculated as log 10 CFU mL^{-1} was assessed both at 24 h and 48 h. Similarly, the medium was also evaluated for pH measurement at 24 h and 48 h using a pH meter (Eutech). Subsequently, the samples were kept at −20 °C until further use.

SCFA quantification using ultra-performance liquid chromatography (UPLC)

The SCFA quantification was performed using UPLC. The methodology explained by Dobrowolska-Iwanek *et al.*, 2020,[24] was followed for SCFA quantification with minor modifications. The cultures were first centrifuged at 8000 rpm for 10 min. Furthermore, the supernatant was withdrawn, acidified to pH 2.5, and then filtered using PVDF 0.45 μm filter (Millipore, USA). Then, the samples were injected to a Waters Acquity UPLC-H system equipped with a STAR RP-18 end-capped column (100 × 2.1 mm, 2 μm particle size) at 25 °C monitored at 210 nm wavelength using an eλ PDA detector. The instrument functioned at a flow rate of 0.2 mL min^{-1} with (A) acetonitrile and (B) 0.1% of *ortho*-phosphoric acid prepared in deionized water, and degassed using an ultrasonicator. The gradient system included: 0 min: A 10%, 3 min: A 20%, 6 min: A 30%, 8 min: A 30%, 12.5 min: A 40%, 14 min: A 80%, 16 min: A 80%, and 18 min: A 10%. After each run, the column was equilibrated for 2 min. The acids were calculated through a comparison of the retention time with the standard. Different dilutions were prepared to determine the calibration curve for the quantification of each acid.

Statistical analysis

Every experiment was done in triplicate, and signified as the mean ± standard deviation. To confirm the accuracy, a two-way Analysis of Variance (ANOVA) with a significance level of $p < 0.05$ was carried out by Tukey's multiple comparison test.

Results and discussion

Effect of the extraction condition on soluble dietary fiber yield

Considering the yield as the assessment index, experiments were performed at varying sample concentrations and extraction methods (Fig. 1A). The extraction was carried out at three concentrations of 2%, 5%, and 10% w/v based on the previous reports[5,25,26] with the maximum SDF yield in 5% samples as A5%, B5%, C5% and D5%, as shown in Fig. 1B. Different extraction conditions have been reported to affect the composition and structure of SDF, positively influencing the concomitant physical and chemical properties.[5] Interestingly, the maximum extraction yield among both mango varieties was observed for HEE at 28.10 ± 0.04% in the A5% sample and 29.26 ± 0.25% in the B5% sample. However, UEE exhibited higher SDF yields for the two pomegranate varieties at 27.74 ± 0.04% (C5%) and 24.43 ± 0.01% (D5%), as shown in Fig. 1B. Fascinatingly, the maximum SDF yield observed in samples A5% and B5% highlights the potential effect of HEE in maximizing the yield. Compared to conventional extraction techniques, homogenization is thought to be a moderate extraction condition that exhibits high yield, continuous production, and an easy industrialization strategy.[5] Furthermore, it has been demonstrated to disrupt the hydrogen bonds that form hemicellulose chains, transforming complex molecules into small-unit polysaccharides.[26] The cellulose hydrolysis produced by the enzymatic activity also reduces the complex polysaccharides to small molecular polysaccharides.[27] In addition, the density and rate of mass transfer probably could have altered the yield. Thereby, the combined effect of treatments and sample concentration enhanced the overall SDF yield. Conversely, the C5% and D5% samples exhibited the maximum SDF yield for UEE (Fig. 1B). The improvement in the SDF yield could possibly be due to the aforementioned effect of EE in conjunction with the breakdown of hydrogen bonds by ultrasonication, which breaks the intricate structures into considerably simpler components. Interestingly, our results are similar to findings reported by Hu *et al.*, 2018,[5] and Dong *et al.*, 2020,[8] where HEE & UEE unveiled maximum SDF yields. It is worth mentioning here that our study summarizes the effect of nine different extraction treatments on the SDF yield from the waste peel of mango and pomegranate. The samples with the maximum yield (*i.e.*, A5% (HEE), was coded further as A5, B5% (HEE) as B5, C5% (UEE) as C5, and D5% (UEE) as D5) were analysed for other structural, techno-functional and prebiotic properties.

Proximate composition

The samples exhibiting the maximum SDF yield (5% w/v) were evaluated for their proximate composition and purity (Table 1). The maximum amount of moisture content was observed as 9.34 ± 0.39% in sample C5. The ash content of all SDF ranged from 9.87% to 10.51%. However, a reduced protein content was observed between 1.05% and 1.28%, which could be ascribed to the enzymatic treatment by proteases, leading to the degradation of proteins. The fat content of all SDF samples was below 1% with a minimum content (0.51%) in sample D5, which is probably due to the sample pre-treatment with ether enhancing purity among the samples.

Functional and other characteristic properties

The functional properties include WAI, WSI, and OAI, representing the hydration properties of the SDF samples. WAI indicates the binding of water that primarily depends on stability, density, chemical structure, amount, nature, and attachment site of SDF. In this study, the WAI of all SDF samples ranged from 4.07 to 7.11 g g^{-1} (Table 2), with significant difference ($p < 0.05$). The reason might be the disintegration of bonds (hydrogen bonds) among hemicellulose, liberating various hydrophilic groups for enhanced binding, along with improved absorption.[26]

Interestingly, in the present study maximum, WAI was observed in sample A5 as 7.11 ± 0.04 g g^{-1} higher than that of apple pomace and papaya peel reported previously.[13,28] The maximum WSI was observed in sample D5 as 69.03 ± 0.73% (Table 2). The enhanced solubility may be attributed to the SDF sample's altered three-dimensional structure and simultaneous increase in the short-chain fiber. The OAI is dependent upon various factors, such as the hydrophobicity of the sample, its charge density and surface property. Thus, the maximum OAI was observed in sample A5 as 4.27 ± 0.08 g g^{-1} (Table 2). The difference in OAI may be attributed to the multifaceted effect of the chemo-mechanical treatment, which breaks down the insoluble fractions, resulting in open functional groups that maximize oil entrapment.[4] The water activity of a sample relies on its moisture content. As presented in Table 2, the water activity of all samples ranged from 0.16 to 0.54, with minimum activity in sample A5. The low water activity exhibits greater stability besides its low susceptibility to degradation by microbes. The EC and ES exhibited significant differences ($p < 0.05$) among all samples, with the maximum EC observed in sample D5 and ES in sample B5, respectively. It is worth mentioning here that the samples exhibited higher EC compared to previously reported literature for citrus dietary fiber and potato pectin, making it a better alternative to commercial emulsifiers with potential health benefits.[26,32]

The other characteristic properties of dietary fiber include GAC, SCBC, CBC, and CEC. The maximum GAC, SCBC, and CBC were observed in samples B5 (8.98 ± 0.01 mg g^{-1}), C5 (5.29 ± 0.08 mg g^{-1}), and B5 (20.91 ± 0.72 mmol g^{-1}), respectively (Table 3). The enhanced activity could be attributed to the combined effect of enzymatic and mechanical treatment, making the structure more loosened and porous, positively correlated to the results of SEM micrographs. This results in all of the non-polar and polar groups being uncovered, making them accessible for interaction and revealing potential health benefits. However, the maximum amount of CEC was observed in sample D5 as 3.05 ± 0.20 mg g^{-1}. Fiber with free functional groups, such as hydroxyl and carboxyl phenols, influences CEC by enhancing the overall chelation characteristic by substituting cations for H^+ ions.[27] Thus, the present study

Table 1 Proximate composition of soluble dietary fiber samples[a]

Sample	Moisture (%)	Fat (%)	Ash (%)	Protein (%)	Purity (%)	SDF (%)
A5	7.58 ± 0.36[a]	0.93 ± 0.11[a]	5.32 ± 0.87[a]	1.05 ± 0.05[a]	85.12 ± 0.32[a]	28.00 ± 0.04[a]
B5	8.51 ± 0.23[a,b]	0.87 ± 0.08[b]	5.33 ± 0.47[b]	1.25 ± 0.02[b]	84.04 ± 0.19[b]	29.26 ± 0.25[b]
C5	9.34 ± 0.39[b]	0.92 ± 0.13[a]	4.68 ± 0.88[c]	1.28 ± 0.05[b]	83.78 ± 0.33[b]	27.74 ± 0.03[a]
D5	9.16 ± 0.48[b]	0.51 ± 0.21[d]	5.12 ± 0.69[c]	1.24 ± 0.05[b]	83.97 ± 0.30[b]	24.43 ± 0.01[d]

[a] Values are the average of three replicates ± SD with significant difference ($p < 0.05$) indicated with different letters (a–d); A5: homogenization-assisted enzymatic extraction (HEE) of SDF from Totapuri, B5: homogenization-assisted enzymatic extraction (HEE) of SDF from Safeda, C5: ultrasonication-assisted enzymatic extraction (UEE) of SDF from Bhagwa, D5: ultrasonication-assisted enzymatic (UEE) extraction of SDF from Daru, SDF: soluble dietary fiber.

Table 2 Functional properties of soluble dietary fiber samples[a]

Sample	WSI (%)	WAI (g g^{-1})	OAI (g g^{-1})	Water activity (a_w)	EC (%)	ES (%)
A5	61.50 ± 0.43[a]	7.11 ± 0.04[a]	4.27 ± 0.08[a]	0.16 ± 0.00[a]	55.00 ± 0.50[a]	53.86 ± 0.66[a]
B5	64.20 ± 0.79[b]	5.07 ± 0.02[b]	3.51 ± 0.08[b]	0.19 ± 0.00[b]	47.66 ± 0.76[b]	67.70 ± 0.70[b]
C5	63.70 ± 0.20[b]	4.07 ± 0.04[c]	3.07 ± 0.03[c]	0.54 ± 0.00[c]	74.83 ± 0.76[c]	59.43 ± 0.56[c]
D5	69.03 ± 0.73[c]	4.79 ± 0.04[d]	3.12 ± 0.01[c]	0.50 ± 0.01[d]	85.50 ± 0.50[d]	47.21 ± 0.64[d]

[a] Values are the average of three replicates ± SD with significant difference ($p < 0.05$) indicated with different letters (a–d); A5: homogenization-assisted enzymatic extraction (HEE) of SDF from Totapuri, B5: homogenization-assisted enzymatic extraction (HEE) of SDF from Safeda, C5: ultrasonication-assisted enzymatic extraction (UEE) of SDF from Bhagwa, D5: ultrasonication-assisted enzymatic extraction (UEE) of SDF from Daru, WSI: water solubility index, WAI: water absorption index, OAI: oil absorption index, EC: emulsion capacity, ES: emulsion stability.

Table 3 Glucose adsorption capacity (GAC), sodium cholate binding capacity (SCBC), cholesterol binding capacity (CBC) and cation exchange capacity (CEC) of extracted soluble dietary fiber samples[a]

Sample	GAC (mg g^{-1})	SCBC (mg g^{-1})	CBC (mmol g^{-1})	CEC (mg g^{-1})
A5	8.00 ± 0.01^{a}	4.31 ± 0.09^{a}	18.47 ± 0.53^{a}	2.05 ± 0.15^{a}
B5	8.98 ± 0.01^{b}	3.95 ± 0.12^{a}	20.91 ± 0.72^{b}	1.95 ± 0.25^{a}
C5	5.33 ± 0.10^{c}	5.29 ± 0.08^{b}	$18.42 \pm 0.14^{a,b}$	2.95 ± 0.23^{b}
D5	6.79 ± 0.03^{d}	5.01 ± 0.06^{c}	$18.67 \pm 0.09^{a,b}$	3.05 ± 0.20^{b}

[a] Values are the average of three replicates ± SD with significant difference ($p < 0.05$) indicated with different letters (a–d); A5: homogenization-assisted enzymatic extraction (HEE) of SDF from Totapuri, B5: homogenization-assisted enzymatic extraction of SDF (HEE) from Safeda, C5: ultrasonication-assisted enzymatic extraction (UEE) of SDF from Bhagwa, D5: ultrasonication-assisted enzymatic extraction (UEE) of SDF from Daru.

Table 4 Sugar profile of soluble dietary fiber samples[a]

Sample code	Glucose (mg g^{-1})	Fructose (mg g^{-1})	Sucrose (mg g^{-1})	Xylose (mg g^{-1})	Raffinose (mg g^{-1})	Inositol (mg g^{-1})
A5	15.43 ± 0.26^{a}	8.76 ± 0.84^{a}	ND	0.24 ± 0.01^{a}	1.18 ± 0.01^{a}	0.26 ± 0.01^{a}
B5	35.22 ± 0.93^{b}	ND	0.43 ± 0.02^{a}	0.26 ± 0.01^{a}	0.07 ± 0.01^{b}	0.25 ± 0.02^{a}
C5	14.14 ± 0.25^{c}	6.05 ± 0.38^{b}	1.17 ± 0.09^{a}	0.05 ± 0.01^{a}	ND	0.18 ± 0.01^{a}
D5	9.78 ± 0.29^{d}	3.54 ± 0.14^{c}	0.48 ± 0.01^{a}	0.57 ± 0.05^{a}	0.26 ± 0.02^{b}	0.26 ± 0.01^{a}

[a] Values are the average of three replicates ± SD with significant difference ($p < 0.05$) indicated with different letters (a–d), ND: not detected.

highlights the imminent role of extracted SDF as a potential health ingredient.

Sugar profile and determination of molecular weight

The monosaccharide composition of all samples was quantified using HPAEC-PAD, as shown in Table 4. Analysis of the SDF samples revealed the presence of various monosaccharides with a maximum content of glucose (35.22 ± 0.01 mg g^{-1}) and minimum of xylose (0.05 ± 0.01 mg g^{-1}) observed in samples B and D, respectively. The most substantial quantity of glucose found in all SDF samples illustrates the effect of the extraction conditions influencing hemicellulose and cellulose, two non-pectic polysaccharides, which results in higher SDF yields and increased glucose content.[8] Similarly, xylose was also observed in all SDF samples. As earlier reported, hemicellulose transformation to oligosaccharides yields xylose as the monomer sugar.[29] Additionally, the occurrence of glucose and xylose have been reported in the side chain of the main pectin backbone.[30] Therefore, this suggests that pectin—the main soluble dietary fiber found in fruit peel—is plausibly present in all SDF samples. The molecular weight determination was carried out to gain structural insights of all SDF samples (Table 5).

Interestingly, there are no reports on the molecular weight determination of extracted soluble dietary fiber using MALDI-TOF/TOF-MS/MS. As depicted in Table 5, all of the SDF samples exhibited varied molecular weight range with different matrices. The two matrices, DHB and THAP, were employed in accordance with previously published studies due to their effective outcomes in the identification of polysaccharides with a wide mass range.[19] The reflectron mode was used for all samples to enhance the resolution of the spectral data of low-mass oligomers (<5000 Da). It was observed that both matrices exhibited similar results in terms of the weight average molecular weight and maximum molecular weight of the SDF samples. The molecular weight of the samples ranged from 103.551 to 1923.382 Da.

The samples exhibited lower molecular weight, which might be due to the ultrasonication treatment disrupting the complex structure and rendering low molecular weight compounds.

Microstructure analysis

SEM is the most valued technique for investigating the microstructure of any material. In the present study, the effect of mechanical and enzymatic treatments was observed on the

Table 5 Molecular weight determination of the soluble dietary fiber samples[a]

Sample	Matrix	M_n	M_w	PI
A5	DHB	195.130	198.906	1.019351
B5		174.252	178.081	1.021974
C5		215.292	216.868	1.00732
		218.497	219.911	1.006471
		199.256	202.235	1.014951
D5		194.295	199.779	1.028225
A5	THAP	209.546	211.598	1.009793
B5		188.125	190.717	1.013778
		378.506	381.219	1.007168
		1563.89	1574.49	1.006778
		1736.04	1740.14	1.002362
C5		223.016	230.845	1.035105
D5		200.450	208.855	1.041931
		153.492	159.972	1.042217

[a] M_n: number average molecular weight, M_w: weight average molecular weight, PI: polydispersity index; A5: homogenization-assisted enzymatic extraction (HEE) of SDF from Totapuri, B5: homogenization-assisted enzymatic extraction (HEE) of SDF from Safeda, C5: ultrasonication-assisted enzymatic extraction (UEE) of SDF from Bhagwa, D5: ultrasonication-assisted enzymatic extraction (UEE) of SDF from Daru.

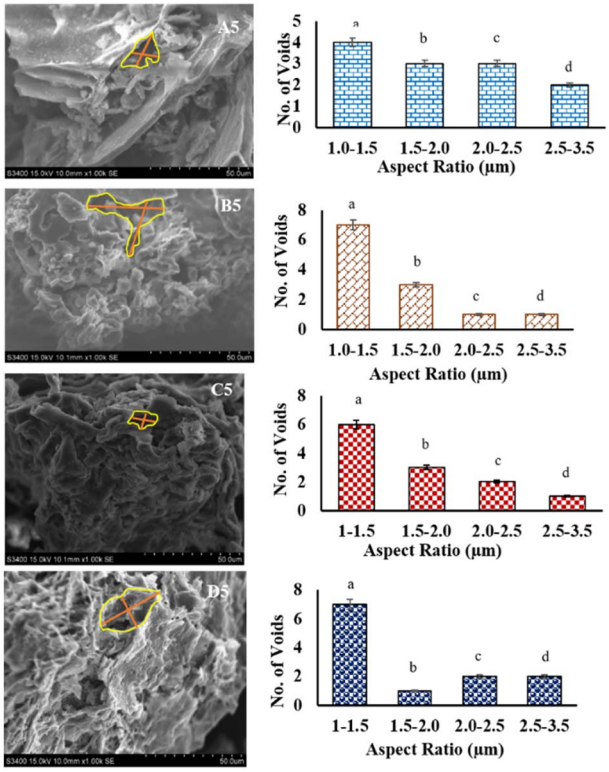

Fig. 2 Microstructure analysis of soluble dietary fiber using scanning electron microscopy. A5: homogenization-assisted enzymatic extraction (HEE) of SDF from Totapuri, B5: homogenization-assisted enzymatic extraction (HEE) of SDF from Safeda, C5: ultrasonication-assisted enzymatic extraction (UEE) of SDF from Bhagwa, D5: ultrasonication-assisted enzymatic extraction (UEE) of SDF from Daru; values are the average of three replicates ± SD with significant difference ($p < 0.05$) indicated with different letters (a–d).

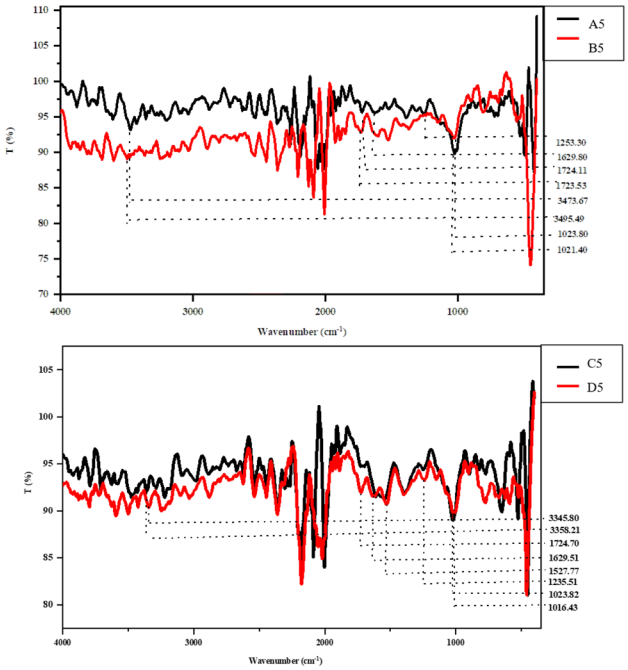

Fig. 3 FT-IR spectra of soluble dietary fiber. A5: homogenization-assisted enzymatic extraction (HEE) of SDF from Totapuri, B5: homogenization-assisted enzymatic extraction (HEE) of SDF from Safeda, C5: ultrasonication-assisted enzymatic extraction (UEE) of SDF from Bhagwa, D5: ultrasonication-assisted enzymatic extraction (UEE) of SDF from Daru.

surface morphology of SDF samples with a maximum SDF yield, *i.e.*, A5, B5, C5, and D5. As seen in Fig. 2, the samples exhibited loosened and porous structures along with voids. The size of the voids was measured using ImageJ software (NIH) with an average void size (μm) for samples A5, B5, C5, and D5 as 1.91 ± 0.64, 1.50 ± 0.54, 1.65 ± 0.57, 1.67 ± 0.74, respectively. In addition, the aspect ratio for the voids was calculated and observed in the range of 1–3.5 μm. This structural distortion may have been caused by the administration of mechanical treatments (ultrasonication and homogenization). These treatments are known to cause turbulence and shear stress, which might lead to the breaking of complex structures. In addition, enzymatic treatment has been reported to make structures porous and loosened, increasing their hydration capacity and making the inner structure more available for binding with water.[23,26] Thereby, in this study, the microstructure analysis unveiled the role of various extraction conditions on morphology, positively correlating to increased techno-functional properties.

FT-IR analysis

The FT-IR spectra help to elucidate the occurrence of various functional groups and the bonding organization, illustrating the structural characteristic of fiber. Thus, the effect of varied extraction conditions was evaluated on the structural characteristics of the SDF samples (Fig. 3). The characteristic band, which spans 3200–3500 cm^{-1}, shows that the –O–H bond is primarily stretched between hemicellulose and cellulose. Out of all of the SDF samples, the B5 and C5 samples showed a red shift of 21.82 cm^{-1} and 12.41 cm^{-1}, respectively.

This peak shift suggested a decrease in intra- and intermolecular hydrogen bonding and an increase in the stretching frequency of the –O–H bond, which had a beneficial impact on the total SDF yield (Fig. 3), demonstrating the plausible influence of extraction conditions on the degradation characteristics of complex polysaccharides.[31] The peaks ranging from 1700 to 1500 cm^{-1} indicate the stretching vibrations amid the aromatic carbon skeleton C=C, ester, and acetyl groups. It is worth mentioning here that a redshift of 0.58 cm^{-1} in the B5 sample, along with the complete disappearance of three peaks in this range, was observed among the B5 and C5 samples, depicting disintegration in the structure of the polysaccharides mainly between hemicellulose and lignin, increasing the overall SDF yields. The distinctive peaks between 1645 and 1612 cm^{-1}, which are mainly found in lignin, explain the C–O stretching between the aromatic or conjugated ketones and flavones.[31] The disappearance of the peak in samples B5 and C5 indicates the effect of extraction conditions in the disintegration of the complex fiber structure, increasing its overall yield. The range from 1400 to 1200 cm^{-1} designates the C–O and C–H stretching, CH_2 bending, and stretching of methyl ester, primarily between pectin, cellulose, and hemicellulose.

Following the previous observation, the complete removal of peaks was observed in this region for samples B5 and C5. Finally, the peaks from 1050 to 1000 cm^{-1} denote the stretching vibrations among –C–O bonds primarily due to collective vibrations among the C–O–C and C–O–H groups.[31] Interestingly, a red shift of 2.4 cm^{-1} and 7.39 cm^{-1} was observed in samples B5 and C5, respectively, clearly depicting the effect of extraction conditions on the increased SDF yield. Therefore, the IR spectra validate the affirmative impact of the extraction conditions on the SDF yield, along with the structural and functional characteristics.

TGA analysis

The thermogravimetric analysis of all SDF samples (A5, B5, C5, and D5) was performed using a TGA analyzer (Fig. 4). The analysis was performed in the 50–400 °C temperature range, unveiling the characteristic degradation and weight loss in the sample. This degeneration could be divided into three main segments at 50–150 °C, 150–250 °C, and 250–400 °C.

The primary stage, ranging from 50 to 150 °C, represents the significant weight loss among all SDF samples ascribed to the evaporation of all of the absorbed water from the samples, degradation of different low molecular weight polysaccharides, along with devolatilization, which mainly occurs at 121 °C.[26] The next stage reveals the loss in sample weight in the range of 150–250 °C. The inception point from where a sudden loss in weight was observed in the degradation characteristics ranged from 152.80 °C to 178.68 °C. However, 20% weight loss among all samples was observed at this stage, with degradation temperatures ranging from 187.07 °C, 199.03 °C, 188.03 °C, and 223.89 °C for samples A5, B5, C5, and D5, respectively. This mass reduction among all samples could be accredited to fiber disintegration *via* reduction, dihydroxylation, or decarboxylation reactions.[12] Comparable results were observed in previous studies, where soluble dietary fiber was extracted from coffee peels, showing a 20% mass reduction in the 130–250 °C temperature range.[8] The final stage, ranging from 250 to 400 °C, resulted in an abrupt weight loss of up to 50% among all SDF samples. The major weight loss among samples A5, B5, C5, and D5 was observed within a temperature range of 293.07 °C, 294.03 °C, 301.03 °C, and 396.89 °C, respectively. The mass degradation might possibly be attributed to the thermal disintegration of hemicellulose, pectin, and lignin. The primary contributor of a mass loss is the pyrolytic disintegration of polysaccharides, especially hemicellulose and pectin.[26] However, the residual masses of all SDF samples A5, B5, C5, and D5 at 398 °C were 39.27%, 36.50%, 43.79%, and 49.97%, respectively. Interestingly, in the present study, a significant residual mass of up to 50% was observed, which indicates the potential thermal stability of all samples. Thus, these results signify the thermal stability of all SDF samples, enhancing its potential application in the food industry.

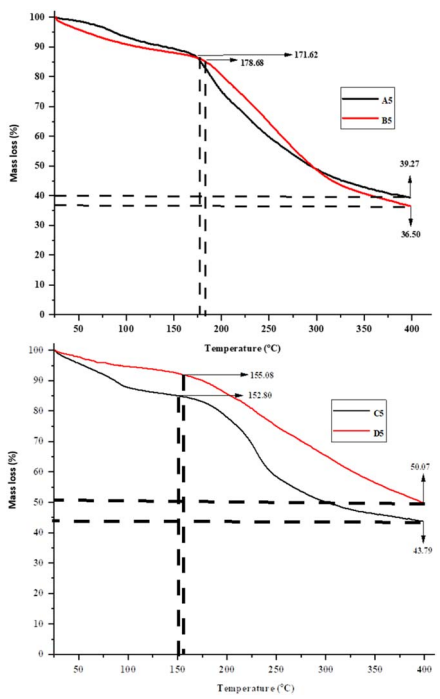

Fig. 4 TGA analysis of the soluble dietary fiber. A5: homogenization-assisted enzymatic extraction (HEE) of SDF from Totapuri, B5: homogenization-assisted enzymatic extraction (HEE) of SDF from Safeda, C5: ultrasonication-assisted enzymatic extraction (UEE) of SDF from Bhagwa, D5: ultrasonication-assisted enzymatic extraction (UEE) of SDF from Daru.

Flavonoid, phenolic content and antioxidant assays

Table 6 describes the TFC and TPC of all SDF samples ranging from 1.71 to 8.57 μg RU per mg, and 5.40 to 10.11 μg GAE per mg, respectively. The results exhibit a significant difference ($p < 0.05$) with lower quantification. The reason for the reduced estimation could be the pretreatment of a peel with 70% ethanol that might have resulted in the leaching of all phytochemicals.[12] Furthermore, prolonged ethanol-induced precipitation and filtration of SDF have been perceived for lower polyphenol concentration.[33] For the estimation of the antioxidant activity, DPPH and ABTS assays were performed with the maximum scavenging activity in sample D (Table 6), which were positively correlated with the results of TPC and TFC.

Color analysis

The color of all samples was quantified in terms of '*L**', '*a**', and '*b**' values with the color difference measured as Δ*E*. As depicted in Table 7, the '*L**' values exhibited significant differences ($p < 0.05$) among them, with maximum lightness in sample A5 (Table 7). Pretreatment of the peel that had possibly eliminated pigments and color could be the most likely cause of the lightness in the samples. The '*a**' values were observed to be significantly different ($p < 0.05$) with positive values among samples C5 and D5. Although no difference was observed for the samples, A5 and B5 represented negative values. The negative value among samples A5 and B5 described the greenness of the sample. The positive values among samples C5 and D5 exhibited the redness in the sample responsible for imparting the overall darkness to the sample and reduced *L** value. However, '*b**' values exhibited a significant difference ($p <$

Table 6 Phenolic, flavonoid and antioxidant activities (DPPH & ABTS) of soluble dietary fiber samples[a]

Sample	Total phenolic content (μg GAE per mg)	Total flavonoid content (μg RU per mg)	IC_{50} of free radical scavenging activities (μg mL^{-1})	
			DPPH	ABTS
A5	5.40 ± 0.38[a]	1.71 ± 0.05[a]	889.59	581.75
B5	2.27 ± 0.09[b]	1.81 ± 0.06[a]	584.87	491.71
C5	6.41 ± 0.44[c]	4.85 ± 0.02[c]	294.48	258.81
D5	10.11 ± 0.06[d]	8.57 ± 0.07[d]	156.76	207.63

[a] Values are the average of three replicates ± SD with significant difference ($p < 0.05$) indicated with different letters (a–d); A5: homogenization-assisted enzymatic extraction (HEE) of SDF from Totapuri, B5: homogenization-assisted enzymatic extraction (HEE) of SDF from Safeda, C5: ultrasonication-assisted enzymatic extraction (UEE) of SDF from Bhagwa, D5: ultrasonication-assisted enzymatic extraction (UEE) of SDF from Daru.

Table 7 Colour values of soluble dietary fiber samples[a]

Sample	L^*	a^*	b^*	ΔE^*
A5	85.43 ± 1.11[a]	−3.35 ± 0.01[a]	8.58 ± 0.14[a]	69.90 ± 1.07[a]
B5	81.94 ± 1.11[b]	−3.31 ± 0.25[a]	12.46 ± 0.16[b]	67.31 ± 0.13[b]
C5	51.33 ± 0.06[c]	0.75 ± 0.02[b]	7.48 ± 0.05[c]	36.48 ± 0.03[c]
D5	48.55 ± 0.02[d]	0.14 ± 0.13[b]	7.35 ± 0.11[c]	33.80 ± 0.03[d]

[a] Values are the average of three replicates ± SD with significant difference ($p < 0.05$) indicated with different letters (a–d); A5: homogenization-assisted enzymatic extraction (HEE) of SDF from Totapuri, B5: homogenization-assisted enzymatic extraction (HEE) of SDF from Safeda, C5: ultrasonication-assisted enzymatic extraction (UEE) of SDF from Bhagwa, D5: ultrasonication-assisted enzymatic extraction (UEE) of SDF from Daru.

0.05), with positive values indicating the yellowness among samples. The color value exhibits a crucial role for application in different food products. Thereby, SDF samples could easily be incorporated into food products exhibiting possible health benefits.

Prebiotic potential

α-Amylase and gastric juice hydrolysis activity. To evaluate the prebiotic potential of all SDF samples, α-amylase and gastric juice hydrolysis activity were carried out. As shown in Table 8, hydrolysis with α-amylase indicated the increased degradation with a simultaneous increase in incubation time, exhibiting a significant difference ($p < 0.05$) among them. However, the maximum hydrolysis of 8.95% was observed in sample C5 at 6 h, with FOS and inulin demonstrating higher hydrolysis of 12.29% and 12.13% after 6 h compared to all SDF samples, respectively. The increased resistance among SDF samples against enzymatic degradation could be attributed to the arrangement of a glycosidic bond within the dietary fiber. Similarly, all SDF samples exhibited an efficient resistance to gastric juice hydrolysis activity with a maximum hydrolysis of 7.73% in the C5 sample after 6 h of incubation (Table 8). In contrast to the SDF samples, FOS and inulin showed increased hydrolysis, with a significant difference ($p < 0.05$) between them. However, the present study exhibited efficient inhibition to hydrolysis by alpha-amylase and gastric juice compared to the previously reported literature by Chen *et al.*, 2020.[34] Thereby, in this study, the higher resistance of the SDF samples substantiated the degradation, remaining intact upon reaching the intestines and thereby validating it as a potential prebiotic source.

pH and cell growth analysis

The prebiotic effect of all SDF samples was further evaluated by fermenting the SDF samples with different probiotics monitored *via* cell growth measurements and pH. The heat map was

Table 8 α-Amylase and gastric juice hydrolysis activity of soluble dietary fiber samples[a]

Time interval	A5	B5	C5	D5	FOS	Inulin
Alpha amylase activity (%)						
0 h	7.23 ± 0.12[a]	6.60 ± 0.01[a]	7.15 ± 0.03[a]	7.05 ± 0.06[a]	7.60 ± 0.03[a]	7.80 ± 0.03[a]
3 h	8.20 ± 0.03[b]	6.73 ± 0.27[a]	8.89 ± 0.06[b]	7.01 ± 0.03[a]	9.52 ± 0.09[b]	8.73 ± 0.04[b]
6 h	8.32 ± 0.04[b]	7.68 ± 0.08[b]	8.95 ± 0.06[b]	7.92 ± 0.06[b]	12.29 ± 0.06[c]	12.13 ± 0.12[c]
Gastric juice hydrolysis activity (%)						
0 h	7.46 ± 0.13[a]	6.64 ± 0.06[a]	7.14 ± 0.03[a]	7.00 ± 0.03[a]	8.76 ± 0.10[a]	8.49 ± 0.17[a]
3 h	7.48 ± 0.09[a]	7.31 ± 0.02[b]	7.40 ± 0.10[a]	7.12 ± 0.12[a]	17.82 ± 0.60[b]	20.28 ± 0.65[b]
6 h	12.77 ± 0.13[b]	7.27 ± 0.09[b]	7.73 ± 0.06[a]	7.73 ± 0.04[b]	55.95 ± 0.06[c]	66.72 ± 0.15[c]

[a] Values are average of replicates ± SD with significant difference ($p < 0.05$) indicated with different letters (a–c); A5: homogenization assisted enzymatic extraction (HEE) of SDF from Totapuri, B5: homogenization assisted enzymatic extraction (HEE) of SDF from Safeda, C5: ultrasonication assisted enzymatic extraction (UEE) of SDF from Bhagwa, D5: ultrasonication assisted enzymatic extraction (UEE) of SDF from Daru, FOS: fructo-oligosaccharide.

drawn to elucidate the effect of probiotic proliferation on both cell growth and pH values. The heat map for cell growth was divided into a six-point scale, starting from less than 6 log10 CFU mL^{-1} as a bluish color and greater than 10 as reddish-orange color. The blue color indicates the minimum cell count range below 6 but not below 5.79 log10 CFU mL^{-1}, and the reddish-orange color indicates the maximum cell count above 10 but not above 10.27 log10 CFU mL^{-1}. In Fig. 5, it is apparent that the SDF samples, along with FOS, supported the growth and proliferation of all probiotic strains. Moreover, glucose and FOS were rapidly metabolized, supporting the proliferation of different probiotic strains at 24 h with a reduction at 48 h. Surprisingly, a substantial increase in the growth of *Lactobacillus plantarum* at 24 h was observed for sample A5, higher than that for glucose and FOS. This signifies the potential role of SDF in the proliferation of different probiotic strains. Interestingly, all SDF samples exhibited effective cell growth ranging between 5.79 log10 CFU mL^{-1} and 10.27 log10 CFU mL^{-1}, illustrating the potential role of extracted SDF samples in the stimulation and proliferation of probiotics.

The pH of the samples exhibited a similar decreasing trend for all SDF samples, along with glucose and FOS (Fig. 5). The heat map was divided into a six-point scale for pH ranges starting from 4.11 to 6.83. The purple color indicates the minimum pH range below 4.5 but not below 4.11, and the bluish color indicates the maximum color above pH 6.5 but not above 7. The decrease in pH for MRS media supplemented with glucose demonstrated a steady decline compared to MRS supplemented with SDF and FOS samples, which is certainly correlated to cell growth measurement. This decrease in pH could be associated with the diverse metabolic pathways of microbes for utilizing the substrate in the media. A substantial decrease in pH could also be caused by catabolic suppression through the use of simple carbon sources like glucose.[34] In addition, the production of various short-chain fatty acids (SCFAs), *i.e.*, propionic, acetic, and butyric acid, during fermentation is mainly responsible for acidification, *i.e.*, pH decrease. Thereby, the results indicate an effective decrease in pH with time that is positively correlated to the cell growth measurement.

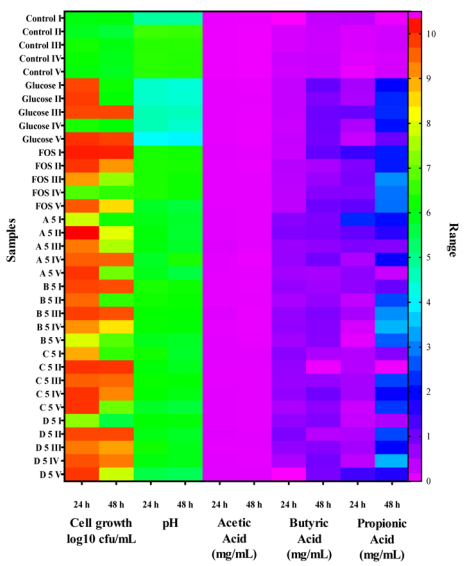

Fig. 5 pH, cell growth and SCFA quantification of SDF samples at 24 and 48 h. A5: homogenization-assisted enzymatic extraction (HEE) of SDF from Totapuri, B5: homogenization-assisted enzymatic extraction (HEE) of SDF from Safeda, C5: ultrasonication-assisted enzymatic extraction (UEE) of SDF from Bhagwa, D5: ultrasonication-assisted enzymatic extraction (UEE) of SDF from Daru, I: *Lactobacillus fermentum*, II: *Lactobacillus plantarum*, III: *Wisella ciberia*, IV: *Lactobacillus brevis*, V: mixed consortium, FOS: fructoligosaccharide.

SCFA quantification

Fig. 5 exemplifies the effect of fermentation on the production of three major SCFAs, *viz.*, acetic, propionic, and butyric acid. The heat map for SCFA quantification was divided into a six-point scale starting from less than 0.128 mg mL^{-1} as purple color and greater than 3.660 mg mL^{-1} as purple-bluish color, where the purple color indicates the minimum SCFA range below 0.128 mg mL^{-1} but not below 0.123 mg mL^{-1}, and the purple-bluish color indicates the maximum SCFA above 3.660 mg mL^{-1} but not above 3.784 mg mL^{-1}. The SDF samples exhibited a significant increase ($p < 0.05$) at 24 h with a slight reduction at 48 h compared to the control samples, demonstrating a positive correlation between the fermentation conditions and SCFA production. The amount of SCFAs produced mainly depends upon the type of carbon source in the testing medium. Interestingly, in the present study, the highest amount of SCFAs produced was propionic acid, followed by acetic and butyric acid. Surprisingly, sample D5, which included the probiotic *Lactobacillus brevis*, showed the highest level of propionic acid (3.57 ± 0.03 mg mL^{-1}) at 24 hours when compared to glucose and FOS, suggesting that it could be a potential source of prebiotics. Similarly, in the case of butyric acid, the highest concentration was observed in the MRS media supplemented with FOS. Interestingly, MRS supplemented with sample C5 containing probiotic *Lactobacillus brevis* unveiled an adequate butyric acid (1.16 ± 0.01 mg mL^{-1}) content acting as an energy source for colonocytes, exhibiting health-associated benefits. However, in the present study, the highest amount of acetic acid (2.64 ± 0.01 mg mL^{-1}) was observed at 24 h for sample A5 containing probiotic *Wisella ciberia*, directing it towards a potential prebiotic candidate. It is worth mentioning here that MRS supplemented with all SDF samples resulted in the maximum progression of almost all probiotic strains (Fig. 5). Therefore, the results emphasize the role of SDF extracted from fruit peels in the proliferation and production of various metabolites. This could be due to the enzymatic and mechanical treatment altering the structural characteristics of SDF samples, affecting its utilization and SCFAs production.[34] Thus, SDF extracted from the waste peel may play a potential role in the amelioration of various inflammatory diseases *via* possible utilization as a prebiotic agent or in innovative synbiotic formulations.

Conclusions

These results highlight the potential role of extraction methods (homogenization and ultrasonication) as an effectual technique

in augmenting the overall structural, thermal, and prebiotic properties of SDF. Thus, the results emphasize the waste valorisation to a value-added ingredient, exhibiting adequate prebiotic activity with potential industrial application. Future research work will explore the opportunity for *in vivo* potential of the SDF candidates in the maintenance of intestinal inflammatory disorders.

Author contributions

Shriya Bhatt: conceptualization, investigation, data curation, roles/writing: original draft. Mahesh Gupta: supervision, roles/writing: original draft.

Conflicts of interest

There are no conflicts to declare.

Acknowledgements

The authors express their gratitude to the Director, CSIR-Institute of Himalayan Bioresource Technology, for their exquisite support. S. B. expresses gratitude to ICMR for awarding a senior research fellowship, ICMR-SRF. The authors also acknowledge Dr Avnesh Kumari (Senior Technical Officer, Biotechnology Division, CSIR-IHBT) and Dr Robin Joshi (Senior Technical Officer, Biotechnology Division, CSIR-IHBT) for SEM and UPLC analysis, respectively, in manuscript number 5168.

Notes and references

1 M. V. Vilariño, C. Franco and C. Quarrington, *Frontiers in Environmental Science*, 2017, **5**, 21.
2 C. M. Ajila, S. G. Bhat and U. P. Rao, *Food Chem.*, 2007, **102**(4), 1006–1011.
3 P. D. Pathak, S. A. Mandavgane and B. D. Kulkarni, *Waste Biomass Valorization*, 2017, **8**, 1127–1137.
4 M. Jia, J. Chen, X. Liu, M. Xie, S. Nie, Y. Chen, J. Xie and Q. Yu, *Food Hydrocolloids*, 2019, **99**, 105349.
5 H. Hu and Q. Zhao, *RSC Adv.*, 2018, **8**(72), 41117–41130.
6 K. Lu, T. Yu, X. Cao, H. Xia, S. Wang, G. Sun, L. Chen and W. Liao, *Front. Nutr.*, 2023, **10**, 1253312.
7 R. Khorasaniha, H. Olof, A. Voisin, K. Armstrong, E. Wine, T. Vasanthan and H. Armstrong, *Food Hydrocolloids*, 2023, **139**, 108495.
8 W. Dong, D. Wang, R. Hu, Y. Long and L. Lv, *Food Res. Int.*, 2020, **136**, 10949.
9 I. Buljeta, D. Šubarić, J. Babić, A. Pichler, J. Šimunović and M. Kopjar, *Appl. Sci.*, 2023, **13**(16), 9309.
10 U. P. Mall and V. H. Patel, *Food Chemistry Advances*, 2023, **2**, 100320.
11 L. Serna-Cock, E. García-Gonzales and C. Torres-León, *Food Rev. Int.*, 2016, **32**(4), 364–376.
12 S. Bhatt and M. Gupta, *Biomass Convers. Biorefin.*, 2022, 1–16.
13 X. Li, X. He, Y. Lv and Q. He, *J. Food Process Eng.*, 2014, **37**(3), 293–298.
14 B. Bello, S. Mustafa, J. S. Tan, T. A. T. Ibrahim, Y. J. Tam, A. B. Ariff, M. Y. Manap and S. Abbasiliasi, *3 Biotech*, 2018, **8**, 1–14.
15 W. Zhang, G. Zeng, Y. Pan, W. Chen, W. Huang, H. Chen and Y. Li, *Carbohydr. Polym.*, 2017, **172**, 102–112.
16 M. A. Kurek, S. Karp, J. Wyrwisz and Y. Niu, *Food Hydrocolloids*, 2018, **85**, 321–330.
17 L. Cheng, X. Zhang, Y. Hong, Z. Li, C. Li and Z. Gu, *Int. J. Biol. Macromol.*, 2017, **101**, 1004–1011.
18 S. Bhatt, N. Kumari, V. Abhishek and M. Gupta, *Journal of Food Measurement and Characterization*, 2021, **15**, 675–685.
19 M. López-García, M. S. D. García, J. M. L. Vilariño and M. V. G. Rodríguez, *Food Chem.*, 2016, **199**, 597–604.
20 R. Kumari, V. Abhishek and M. Gupta, *Vegetos*, 2021, **34**, 205–211.
21 S. Bhatt, V. Dadwal, Y. Padwad and M. Gupta, *J. Food Process. Preserv.*, 2022, **46**(1), e16137.
22 S. Bhatt, B. Singh and M. Gupta, *J. Agric. Food Res.*, 2020, **2**, 100069.
23 G. J. Chen, Q. Y. Hong, N. Ji, W. N. Wu and L. Z. Ma, *Int. J. Biol. Macromol.*, 2020, **155**, 674–684.
24 J. Dobrowolska-Iwanek, R. Lauterbach, H. Huras, P. Paśko, E. Prochownik, M. Woźniakiewicz, S. Chrząszcz and P. Zagrodzki, *Microchem. J.*, 2020, **155**, 104671.
25 J. Gan, Z. Huang, Q. Yu, G. Peng, Y. Chen, J. Xie, S. Nie and M. Xie, *Food Hydrocolloids*, 2020, **101**, 105549.
26 Y. Zhang, J. Liao and J. Qi, *Lwt*, 2020, **128**, 109397.
27 Y. Jiang, H. Yin, Y. Zheng, D. Wang, Z. Liu, Y. Deng and Y. Zhao, *Food Res. Int.*, 2020, **136**, 109348.
28 K. Wang, M. Li, Y. Wang, Z. Liu and Y. Ni, *Food Hydrocolloids*, 2021, **110**, 106162.
29 L. C. Rojas-Pérez, P. C. Narváez-Rincón, M. A. M. Rocha, E. Coelho and M. A. Coimbra, *Bioresources and Bioprocessing*, 2022, **9**(1), 105.
30 J. Müller-Maatsch, M. Bencivenni, A. Caligiani, T. Tedeschi, G. Bruggeman, M. Bosch, J. Petrusan, B. Van Droogenbroeck, K. Elst and S. Sforza, *Food Chem.*, 2016, **201**, 37–45.
31 N. George, A. A. Andersson, R. Andersson and A. Kamal-Eldin, *NFS J.*, 2020, **21**, 16–21.
32 J. S. Yang, T. H. Mu and M. M. Ma, *Food Chem.*, 2018, **244**, 197–205.
33 G. Yu, J. Bei, J. Zhao, Q. Li and C. Cheng, *Food Chem.*, 2018, **257**, 333–340.
34 G. J. Chen, Q. Y. Hong, N. Ji, W. N. Wu and L. Z. Ma, *Int. J. Biol. Macromol.*, 2020, **155**, 674–684.